catalysts

MDPI

Article

DFT Study on Mechanisms of the N_2O Direct Catalytic Decomposition over Cu-ZSM-5: The Detailed Investigation on NO Formation Mechanism

Congru Gao, Jianwei Li *, Jie Zhang * and Xiuliang Sun

State Key Laboratory of Chemical Resource Engineering, Beijing University of Chemical Technology, Beijing 100029, China; gaocr@mail.buct.edu.cn (C.G.); sunxl@mail.buct.edu.cn (X.S.)

* Correspondence: lijw@mail.buct.edu.cn (J.L.); zhangjie@mail.buct.edu.cn (J.Z.); Tel.: +86-1361-105-3831 (J.L.); +86-1800-113-7991 (J.Z.)

Received: 23 April 2020; Accepted: 6 June 2020; Published: 9 June 2020

Abstract: Nitrous oxide (N_2O) is an industrial emission that causes the greenhouse effect and damages the ozone layer. Density functional theory study on the N_2O direct catalytic decomposition over Cu–ZSM-5 has been performed in this paper. Two possible reaction mechanisms for N_2O direct catalytic decomposition over Cu-ZSM-5 were proposed (O_2 formation mechanism and Nitric oxide (NO) formation mechanism). The geometrical parameters, vibration frequency and thermodynamic data of the intermediate states in each step have been examined. The results indicate that N_2O can be adsorbed on active site Cu in two ways (O-terminal or N-terminal), and N_2O decomposition reactions can occur in both cases. The NO formation mechanism exhibits higher N_2O dissociation reaction due to lower energy barrier.

Keywords: DFT; Cu-ZSM-5; N_2O direct catalytic decomposition

1. Introduction

Nitrous oxide (N_2O) is an important pollutant that can cause the greenhouse effect, and it is expected that the global temperature will rise by 0.3K for every doubling of N_2O concentration in the atmosphere [1]. At the same time, N_2O will destroy ozone in the atmosphere and form acid rain, which will undoubtedly seriously damage the human living environment [2]. Human activities (combustion of coal in fluidized-bed reactors, industrial production of adipic acid and nitric acid, automobile emissions, etc.) are the main causes of imbalance of N_2O in the atmosphere [3]. Controlling N_2O emissions and developing N_2O treatment technologies as soon as possible are particularly important to protect human living environment.

Through N_2O direct catalytic decomposition process, the N_2O molecule is directly decomposed to form O_2 and N_2 at a relatively low temperature (300–700 °C). This process has the significant advantages of high conversion rate (>99%), low cost, no secondary pollution, and simple operation [4,5].

Exploring catalysts, with high activity and high thermal stability, has become one of the research hotspots nowadays. As the high specific surface area, the unique pore structure, and the excellent N_2O decomposition activity, zeolites have been extensively studied [5–10]. It is reported that the metal cation exchanged ZSM-5 showed high catalytic activity [9,11–13]. The Cu-ZSM-5 has aroused widespread concern because of its high selectivity and activity, many researchers have devoted themselves to this field, and they have obtained many research reports on the preparation and performance of Cu-ZSM-5 for the N_2O direct catalytic decomposition process [3,5,14–16].

Many methods have been used to investigate the N_2O decomposition mechanism over Cu-ZSM-5 catalyst. Marijke's group [17] presented a first practice of operando UV–vis diffuse reflectance spectroscopic technique to study the decomposition of NO and N_2O over Cu-ZSM-5. They observed the role of the bis(μ-oxo) dicopper core in the catalytic decomposition process and found that the O2 release step limits the N_2O decomposition speed. Kapteijn's group [18] developed a detailed micro kinetic model to predict the N_2O catalytic decomposition over Co-, Fe-, and Cu-ZSM-5 catalysts. Through this model, they found that the O atom of N_2O combines with the active center and transfers to form O_2 in the next step. At the same time, they proved that this reaction is inhibited by O_2 from the view of kinetics.

Quantum chemical calculation is an effective theoretical method to deeply study the structure and energy changes of substances during the reaction [19–25]. Some computer Simulation studies were undertaken on M-ZSM-5 (where M = Fe, Cu, Co, etc.) catalysts and N_2O decomposition, to clarify the reaction mechanism and thermodynamics [26–29]. Lund's group [30] studied the catalytic decomposition process of N_2O on different Fe-ZSM-5 density functional theory(DFT) models (24T double-layer annular model and 5T model), and found that the 24T model has a decomposition reaction energy barrier similar to the 5T model. Therefore, the authors propose that a 5T model, without considering that the pore effect can obtain sufficiently accurate results for calculating the energy barrier of N_2O catalytic decomposition. Fellah and Onal [31] investigated the cluster surfaces and channel cluster of Fe-ZSM-5 and Co-ZSM-5. They found that the calculated Co-ZSM-5 activation energy barrier was lower than that of Fe-ZSM-5, and both catalysts are limited by the process of O_2 desorption. Liu et al. [26] made a lot of efforts in their simulation study on the N_2O catalytic decomposition, they have drawn a Cu-ZSM-5 catalytic route map extended from Fe-ZSM-5 and Co-ZSM-5. They pointed out that the N_2O adaptation mechanism is similar to Fe-ZSM-5 and Co-ZSM-5. However, the N_2O decomposition mechanism is different. Chen's group [27] investigated the N_2O decomposition over Fe-Beta, which provides us with another possible type of reaction mechanism (nitric oxides (NO) formation mechanism) with N_2O adsorption by N atom.

Nevertheless, there are still some deficiencies in the results of previous studies. In the first place, when the by-products as nitrogen oxides appear during the catalytic reaction, the decomposition mechanism of N_2O is much more complicated than estimated [28]. In the second place, there is a lack of energy data of transition states, and a lack of comparison between different reaction pathways and mechanisms.

For this study, our purpose is to discuss two possible mechanisms for the N_2O dissociation, and focus on the structure of the intermediate products, the vibration frequency of the transition states, and the thermodynamic data. By calculating the energy barrier of each reaction process, the rate-limiting step of the process is determined.

2. Results

Two possible types of reaction mechanisms for nitrous oxide direct catalytic decomposition are proposed based on the 5T Cu-ZSM-5 model, including O_2 formation mechanism (Scheme 1a) and NO formation mechanism (Scheme 1b). The Cu-ZSM-5 is labeled as Cu-Z, each transition state in the reaction is marked as TS, and the IM is the short for intermediate. The symbol Cu-Z-N_2O or symbol Cu-O-Z-N_2O represents N_2O molecule adsorbs on the active site using the O-terminal respectively, and the symbol Cu-O-Z-N_2O' means N_2O molecule is adsorbed to αO through the N-terminal. Figure 1 shows the optimization models used to study the direct decomposition mechanism of N_2O in DFT calculation and the schematic diagram of the reaction steps of the two mechanisms.

- Part A1

Cu-Z + N_2O----Cu-Z-N_2O	Step A1
Cu-Z-N_2O----Cu-Z-N_2O-TS	Step A2
Cu-Z-N_2O-TS---- Cu-O-Z-N_2	Step A3
Cu-O-Z-N_2----Cu-O-Z+N_2	Step A4

- Part A2

Cu-O-Z+N_2O----Cu-O-Z-N_2O	Step A5
Cu-O-Z-N_2O----Cu-O-Z-N_2O-TS	Step A6
Cu-O-Z-N_2O-TS---- Cu-O_2-Z-N_2	Step A7
Cu-O2-Z-N_2----Cu-O_2-Z+N_2	Step A8

- Part A3

Cu-O_2-Z----Cu-Z+O_2	Step A9

(**a**)

- Part B1

Cu-O-Z + N_2O----Cu-O-Z-N_2O'	Step B1
Cu-O-Z-N_2O' ---- Cu-O-Z-N_2O' -TS1	Step B2
TS1 ---- Cu-Z-$(NO)_2$	Step B3

- Part B2

Cu-Z-$(NO)_2$ ----TS2	Step B4
TS2 ----Cu-Z-NO-NO	Step B5

- Part B3

Cu-Z-NO-NO----Cu-Z-NO+NO	Step B6

(**b**)

Scheme 1. Reaction steps of the O_2 formation mechanism (**a**); Reaction steps of the NO formation mechanism (**b**).

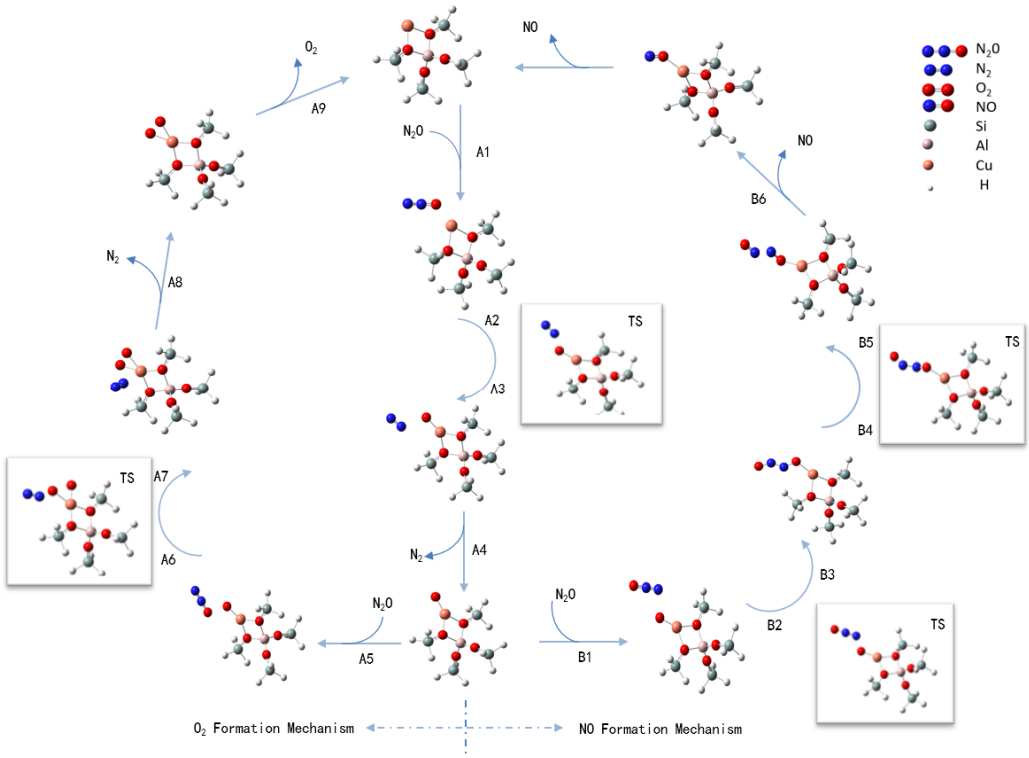

Figure 1. Optimized models and the schematic diagrams of the reaction steps of the two mechanisms.

The energy profile of each mechanism and the partially optimized geometric parameters of the model in each reaction step are marked in Figure 2a,b. Table S1 shows the detailed geometric parameters of each optimized model, in which N and O atoms have been noted (O1–N1–N2 for the first N_2O, O2–N2–N3 for the second N_2O, and N1–O1 for NO). Table S2 shows the DFT energy calculation results for each reaction step.

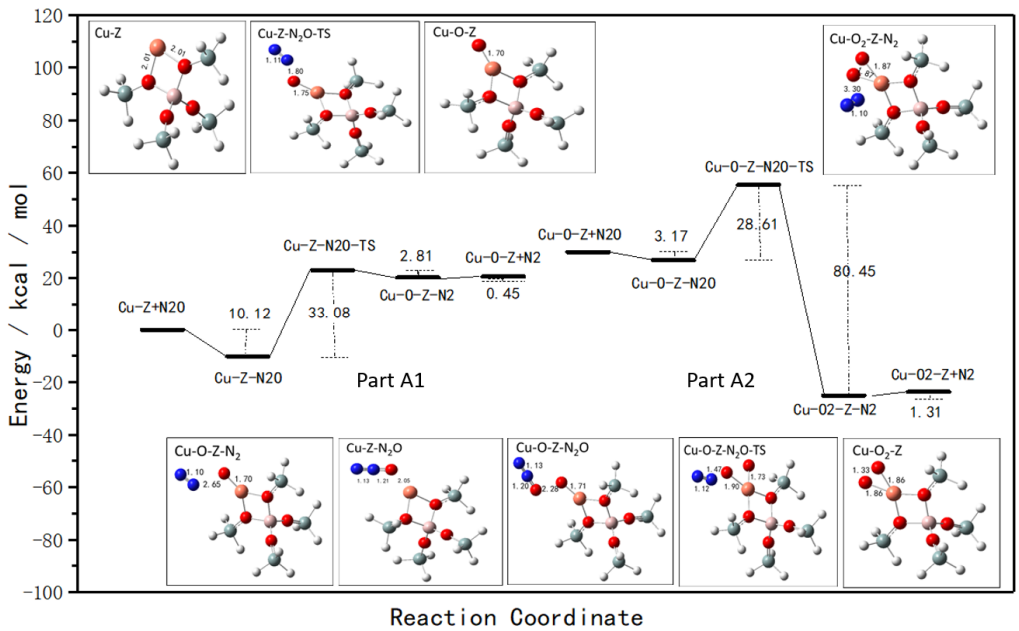

(**a**)

Figure 2. *Cont.*

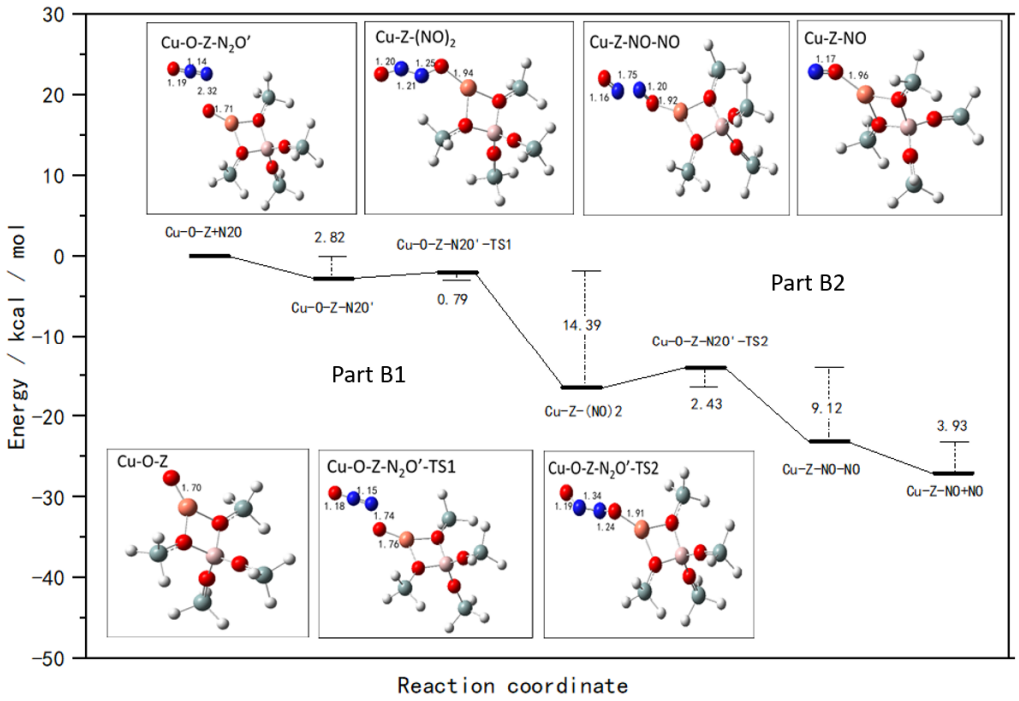

(**b**)

Figure 2. Energy profile for O_2 formation mechanism (**a**); Energy profile for NO formation mechanism (**b**).

2.1. Formation Mechanism of O_2 Based on DFT Calculations

As shown in Scheme 1a, the O_2 formation mechanism includes three parts (Part A1–Part A3) and nine steps (Step A1–Step A9), Part A1 describes the first N_2O molecule catalytic decomposition process, Part A2 explains the second N_2O molecule decomposition, and Part A3 shows the process of O_2 desorption.

2.1.1. Part A1

Reaction step A1 shows a process in which the first N_2O molecule adsorbs on the active site using the O-terminal. The adsorption energy reaches −10.12 kcal/mol, which means that the N_2O molecule can easily adsorb on the Cu and releases a small amount of heat. Since the adsorption energy is low, reverse reaction (N_2O desorption) may also occur under the reaction conditions, so step A1 can be considered as a reversible adsorption step of N_2O.

Reaction step A2 describes the process from N_2O adsorption state to the first TS, which is the key-step in Part A1. The reaction energy barrier (ΔE) is 33.08 kcal·mol^{-1}, which indicates that the reaction needs to absorb lots of heat to reach the TS. The structural parameters of the TS are as follows; the bond length of Cu–ON_2 is 1.75Å, the bond length of O–N_2 is 1.80Å, the bond length of N-N is 1.11Å, and the N_2O bond angle is changed from adsorption state's 177.9° to 143.7°. The imaginary frequency of the TS is 294.61 icm^{-1}, which is confirmed by intrinsic reaction coordinate (IRC) path analysis.

Reaction step A3 has a small negative reaction energy change (−2.81 kcal·mol$^{-1)}$, the reaction can proceed automatically, and the O–N_2 is broken to form highly active αO and adsorbed N_2. Then in step A4, N_2 is desorbed, and a small amount of heat energy (ΔE = 0.45 kcal·mol^{-1}) is absorbed.

2.1.2. Part A2

Part A2 exhibits the second N_2O molecule catalytic decomposition process. During reaction step A5, N_2O adsorbs on the Cu center through the O-terminal. This step's reaction energy barrier is −3.17 kcal mol^{-1}, which is as reversible as in step A1.

Reaction step A6 demonstrates the second key-step. It has a lager reaction energy barrier (28.61 kcal mol^{-1}). The structural parameters of the TS are as follows: the bond length of Cu–ON_2 is 1.90Å, the bond length of O–N2 is 1.47Å, the bond length of N–N is 1.12Å, and the bond angle of O2–N3–N4 is 149.6°. The imaginary frequency of the TS is 799.38 icm^{-1}, which is determined by IRC path analysis.

Reaction step A7 explains the process of O–N2 bond cleavage and adsorbed N_2 formation. This step releases a large amount of heat, when ΔE reaches −80.45 kcal·mol^{-1}. In a while, N_2 desorbs (step A8) despite the low energy (1.31 kcal·mol^{-1}).

2.1.3. Part A3

The last step of Part A shows the O_2 desorption process, this step's energy barrier is 33.59 kcal mol^{-1}. This result means that the step A9 comes to be the speed-determining step of the whole reaction process.

2.2. Formation Mechanism of NO Based on DFT Calculations

As described above, the difference between the formation mechanism of NO and that of O_2 is the second N_2O molecule adsorption method. Therefore, this section focuses on the second N_2O molecule catalytic decomposition process which is named NO formation mechanism. As shown in Scheme 1b, it consists of three parts (Part B1–Part B3).

2.2.1. Part B1

Part B1 describes the process from the second N_2O adsorption state (through the N-terminal) to the transition state. Eventually, an intermediate product (IM) is created. Reaction step B1 explains that the second N_2O adsorbs on the αO through the N-terminal process, and this step has a small adsorption energy (2.81 kcal·mol^{-1}). The bond length of αO–N_2O is 2.32Å, and the bond angle of O2–N3–N4 is 179.9°.

Reaction step B2 shows the process of the first TS (Cu–O–Z–N_2O'–TS) formation, which absorbs a small amount of energy (0.79 kcal·mol^{-1}). The bond angle of O2–N3–N4 changes a little, but the bond length of O1–N4 decreases rapidly. The imaginary frequency of the TS is 241.10 icm^{-1}, which is also confirmed by IRC path analysis. When the reaction (Reaction step B3) proceed from TS to IM, it carries on automatically and releases energy (14.39 kcal·mol^{-1}).

2.2.2. Part B2

Part B2 demonstrates the process from IM to Cu–Z–NO–NO. The reaction step B4 shows the path from IM to the second TS. This step, which is identified by the experimental results as a reaction rate-determining step, shows a tiny energy barrier (2.43 kcal·mol^{-1}). The TS's imaginary frequency value is 280.03 icm^{-1}. During the process, the bond angle of O2–N3–N4 has been changed to 125.8°. The energy change of reaction step B5 (Cu–O–Z–N_2O'–TS2 to Cu–Z–NO–NO) is 9.12 kcal·mol^{-1}, and it will perform automatically.

2.2.3. Part B3

Part B3 is the reaction process of the desorption of adsorbed NO, the release of NO and the formation of Cu-Z-NO. This automatic reaction step releases a small amount of energy.

3. Discussion

Summarizing the models constructed above, two different types of reaction mechanisms are discussed. When N_2O directly decomposes following the O_2 formation mechanism, both N_2O molecules adsorb on the active site using the O-terminal. In this work, the whole reaction process is divided into three parts: The first N_2O adsorbs on the active center Cu and produces N_2 with reaction, the second N_2O molecule adsorbs on active center Cu and reacts to release N2, and the two O

atoms combine to form O_2 and desorb from the catalyst. The three parts of the reaction process have shown three energy barriers (33.08 kcal·mol^{-1}, 28.61 kcal·mol^{-1}, and 33.59 kcal·mol^{-1}, respectively). Considering the entire reaction process, the speed-limiting step of the mechanism is O_2 desorption, which has been widely recognized in the literature [26,29]. When Kapteijn's group [18] conducted an experiment on the N_2O decomposition process over M-ZSM-5 (Where M = Co, Fe, and Cu), they found that the process of N_2O decomposition, based on the Cu-ZSM-5, has an apparent activation energy of 32.5 ± 9.1 kcal/mol (136 ± 8 KJ·mol^{-1}), which is highly consistent with this study. Liu et al. [26] analyzed the decomposition reactions of three N_2O molecules in a sequence based on a similar simulation calculation Cu-ZSM-5 model and verified that the reaction energy barrier value reached 39.48 kcal/mol. Table 1 shows the comparison of energy barrier from part A1 to part A3. They also listed optimized geometric parameters and energy data of the transition state, consistent with present study, but those are not comprehensive and specific enough. Through the study of the O_2 formation mechanism by DFT, an effective calculation model is established, a reliable calculation method is verified, and more complete optimized geometric parameters and transition state energy data are given in Tables S1 and S2.

Table 1. Energy barrier comparison of the Part A1–A3.

Part	Energy Barrier/ kcal·mol^{-1}	Energy Barrier [30]/ kcal·mol^{-1}
A1	33.08	35.18
A2	28.61	28.07
A3	33.59	39.48

As the other important part of this study, we discussed the NO formation process of N_2O catalytic decomposition reaction using 5T Cu-ZSM-5 model. Mechanism design referred to the experimental research results in the literatures [27,28,32–34]. We found that NO was generated due to the N–NO bond broken during the second N_2O adsorption process, and the NO formation mechanism reaction has higher activity than the O_2 formation mechanism reaction. Zhang's group [35] pointed out that the structure of the O-terminal N_2O molecule is more stable than that of the N-terminal N_2O molecule over Cu-ZSM-5, but the conclusion over other zeolites is opposite. Chen' s group [27] conducted a DFT study on the two types of formation mechanisms over Fe-beta. The energy barriers of the two types of formation mechanisms are contrary to those over Cu-ZSM-5. Table 2 shows the comparison results of energy barrier during the second N_2O molecule decomposition process. This result may explain why O_2 does not counteract the N_2O direct catalytic decomposition reaction using Cu-ZSM-5 zeolite, and more by-products are formed during the catalytic process.

Table 2. Energy barrier comparison of the second N_2O molecule decomposition process.

Mechanism	Energy Barrier/ kcal·mol^{-1}	Energy Barrier [31]/ kcal·mol^{-1}
O_2 formation mechanism	28.61	35.78
NO formation mechanism	0.79	26.92

4. Experimental and Computational Methods

In the present work, the DFT-based quantum chemistry was used to investigate the N_2O direct catalytic decomposition mechanisms over Cu-ZSM-5. ZSM-5 zeolite structure model is cut out from the molecular structure database in Material Studio 4.0 software, and the cluster concerned is the 5T model [(SiH3)4AlO4Cu] shown in Figure 3b. The Al atom in the 5T model falls at the T12 site (Figure 3a), because the Si atom at T12 site is the most easily replaced by Al atom based on published literature [36,37]. A Cu+ ion compensate the Al atom and form the active site. H atoms are used to balance the boundary charge. All atoms in the calculation are relaxed.

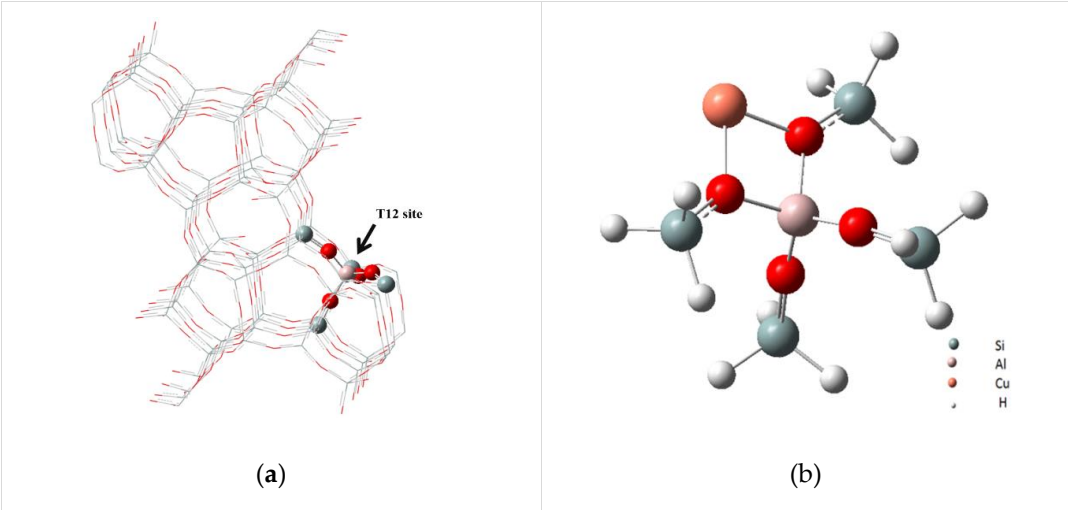

Figure 3. Structure diagram of the computational model. (**a**) Location of the Al atom within the crystal structure of ZSM-5; (**b**) optimized 5T model of Cu-ZSM-5.

Gaussian-09 software package (Gaussian 09, Revision A.02, Gaussian, Inc., Wallingford, CT, USA, 2016) was used for all the simulate calculations in this paper [38–42]. B3LYP method (Becke's three-parameter hybrid, Lee-Yang-Parr's correlation function) was used [43,44]. In the simulation study of geometry optimization and transition state search, the LANL2DZ basis set was used to describe the atomic Cu, and the 6-31G(d) basis set was used for the other atoms (Al, Si, N, O and H). However, the 6-311++G (d, p) set was applied for energy change calculations on top of the structural optimization results to calculate the energy barrier values [45–47]. In the frequency calculation, zero-point energy (ZPE) was used for energy correction [48–53].

5. Conclusions

During the present work, we have simulated two mechanisms of the N_2O direct catalytic decomposition, and proposed the structure parameters, vibration frequency and thermodynamic data of the intermediate states in each step using DFT calculations. The most important discovery of this work is to provide us with a theoretical calculation evidence showing that N_2O molecular can adsorb on Cu−O−Z through both O terminal and N terminal and form O_2 or NO, respectively. The O_2 desorption step is the speed-limit step for O_2 formation mechanisms, and the path from IM to the second TS (Cu–O–Z–N_2O'–TS2) turns out to be the speed-limit step of NO formation mechanisms. The latter showed high N_2O dissociation activity due to a much lower energy barrier.

Supplementary Materials: The following are available online at http://www.mdpi.com/2073-4344/10/6/646/s1, Table S1. Structural parameters (diameter in Å, angle in o) of optimized models, Table S2. Energy results of each step for O2 formation mechanism and NO formation mechanism.

Author Contributions: Writing—original draft preparation, C.G.; supervision, J.L.; writing—review and editing, J.Z.; methodology, X.S. All authors have read and agreed to the published version of the manuscript.

Funding: This research was funded by National Key Research and Development Project, grant number 2017YFC0210905.

Conflicts of Interest: The authors declare no conflict of interest.

References

1. Watson, R.T.; The Core Writing Team. *Climate Change 2001: Synthesis Report. A Contribution of Working Groups I, II, and III to the Third Assessment Report of the Intergovernmental Panel on Climate Change*; Cambridge University Press: Cambridge, UK; New York, NY, USA; 398p.
2. Dickinson, R.E.; Cicerone, R.J. Future global warming from atmospheric trace gases. *Nature* **1986**, *319*, 109–115. [CrossRef]
3. Ram, P.J.; Kapteijn, F.; Schöffel, K.; Moulijn, J.A. Formation and control of N_2O in nitric acid production: Where do we stand today. *Appl. Catal. B* **2003**, *44*, 117–151.
4. Armor, J.N.; Braymer, T.A.; Farris, T.S.; Li, Y.; Petrocelli, F.P.; Weist, E.L.; Kannan, S.; Swamy, C.S. Calcined hydrotalcites for the catalytic decomposition of N_2O in simulated process streams. *Appl. Catal. B* **1996**, *7*, 97–406. [CrossRef]
5. Kapteijn, F.; Mirasol, R.J.; Moulijn, J.A. Heterogeneous catalytic decomposition of nitrous oxide. *Appl. Catal. B* **1996**, *9*, 25–64. [CrossRef]
6. Liu, N.; Zhang, R.; Chen, B. Comparative study on the direct decomposition of nitrous oxide over M (Fe, Co, Cu)–BEA zeolites. *J. Catal.* **2012**, *294*, 99–112. [CrossRef]
7. Shen, Q.; Li, L.; Hao, Z.; Xu, Z. Highly active and stable bimetallic Ir/Fe–USY catalysts for direct and NO–assisted N_2O decomposition. *Appl. Catal. B* **2008**, *84*, 734–741.
8. Pirngruber, G.D.; Frunz, L.; Pieterse, J.A. The synergy between Fe and Ru in N_2O decomposition over FeRu—FER catalysts: A mechanistic explanation. *J. Catal.* **2006**, *243*, 340–349. [CrossRef]
9. Smeets, J.P.; Groothaert, H.M.; Teeffelen, R.M. Direct NO and N_2O decomposition and NO—Assisted N_2O decomposition over Cu—Zeolites: Elucidating the influence of the Cu—Cu distance on oxygen migration. *J. Catal.* **2007**, *245*, 358–368. [CrossRef]
10. Xu, X.; Xu, H.; Kapteijn, F.; Moulijn, J.A. SBA-15 based catalysts in catalytic N_2O decomposition in a model tail—Gas from nitric acid plants. *Appl. Catal. B* **2004**, *53*, 265–274. [CrossRef]
11. Yu, J.; Xu, R. Rational approaches toward the design and synthesis of zeolitic inorganic open-framework materials. *Acc. Chem. Res.* **2010**, *43*, 1195–1204. [CrossRef]
12. Chang, Y.F.; McCarty, J.G.; Washsman, E.D.; Wong, V.L. Catalytic decomposition of nitrous oxide over ru-exchanged zeolites. *Appl. Catal. B* **1994**, *4*, 283–299. [CrossRef]
13. Lisi, L.; Pirone, R.; Russo, G.; Santamaria, N.; Stanzione, V. Nitrates and nitrous oxide formation during the interaction of nitrogen oxides with Cu-ZSM-5 at low temperature. *Appl. Catal. A* **2012**, *413–414*, 117–131. [CrossRef]
14. Upakul, D.; Ines, L.; Weckhuysen, B.M.; Beale, A. Local environment and nature of Cu active sites in zeolite-based catalysts for the selective catalytic reduction of NO_x. *ACS Catal.* **2013**, *3*, 413–427.
15. Lucas, A.D.; Valverde, J.L.; Dorado, F.; Romero, A.; Asencio, I. Influence of the ion exchanged metal (Cu, Co, Ni and Mn) on the selective catalytic reduction of NO_X over mordenite and ZSM-5. *J. Mol. Catal. A* **2005**, *225*, 47–58. [CrossRef]
16. Perez-Ramirez, J.; Berger, R.J.; Mul, G.; Kapteijn, F.; Moulijn, J.A. The six-flow reactor technology: A review on fast catalyst screening and kinetic studies. *Catal. Today* **2000**, *60*, 93–109. [CrossRef]
17. Groothaert, M.H.; Lievens, K.; Leeman, H.; Weckhuysen, B.M.; Schoonheydt, R.A. An operando optical fiber UV–vis spectroscopic study of the catalytic decomposition of NO and N_2O over Cu-ZSM-5. *J. Catal.* **2003**, *220*, 500–512. [CrossRef]
18. Kapteijn, F.; Marban, G.; Rodriguez-mirasol, J.; Moulijn, J.A. Kinetic analysis of the decomposition of nitrous oxide over ZSM-5 catalysts. *J. Catal.* **1997**, *167*, 256–265. [CrossRef]
19. Walter, T. Computational catalysis-past, present, and future. *Angew. Chem. Int. Ed.* **2014**, *53*, 8605–8613.
20. Pidko, E.A. Toward the balance between the reductionist and systems approaches in computational catalysis: Model versus method accuracy for the description of catalytic systems. *ACS Catal.* **2017**, *7*, 4230–4234. [CrossRef]
21. Sameera, W.M.C.; Maseras, F. Transition metal catalysis by density functional theory and density functional theory/molecular mechanics. *Wires Comput. Mol. Sci.* **2012**, *2*, 375–385. [CrossRef]
22. Cramer, C.J.; Truhlar, D.G. Density functional theory for transition metals and transition metal chemistry. *Phys. Chem. Chem. Phys.* **2009**, *11*, 10757–10816. [CrossRef] [PubMed]

23. Esposito, R.; Raucci, U.; Cucciolito, M.E.; Guida, R.D.; Scamarella, C.; Rega, N.; Ruffo, F. Iron(III) complexes for highly efficient and sustainable ketalization of glycerol: A combined experimental and theoretical study. *ACS Omega* **2019**, *4*, 688–698. [CrossRef] [PubMed]
24. Fellah, M.F.; Onal, I. Direct methane oxidation to methanol by N_2O on Fe- and Co-ZSM-5 clusters with and without water: A density functional theory study. *J. Phys. Chem. C* **2010**, *114*, 3042–3051. [CrossRef]
25. Woertink, J.S.; Smeet, P.J.; Groothaert, M.H.; Vance, M.A.; Sels, B.F.; Schoonheydt, R.A.; Solomon, E.I. A $[Cu_2O]^{2+}$ core in Cu-ZSM-5, the active site in the oxidation of methane to methanol. *Proc. Natl. Acad. Sci.* **2009**, *106*, 18908–18913. [CrossRef] [PubMed]
26. Liu, X.; Yang, Z.; Zhang, R.; Li, Q.; Li, Y. Density functional theory study of mechanism of N_2O decomposition over Cu-ZSM-5 zeolites. *J. Phys. Chem. C* **2012**, *116*, 20262–20268. [CrossRef]
27. Chen, B.; Liu, N.; Liu, X.; Zhang, R.; Li, Y.; Li, Y.; Sun, X. Study on the direct decomposition of nitrous oxide over Fe-beta zeolites: From experiment to the theory. *Catal. Today* **2011**, *175*, 245–255. [CrossRef]
28. Zhang, R.; Liu, N.; Lei, Z.; Chen, B. Selective transformation of various nitrogen-containing exhaust gases toward N_2 over zeolite catalysts. *Chem. Rev.* **2016**, *116*, 3658–3721. [CrossRef]
29. Mul, G.; Perez-Ramirez, J.; Kapteijn, F.; Moulijn, J.A. NO assisted N_2O decomposition over ex-framework FeZSM-5: Mechanistic aspects. *Catal. Lett.* **2001**, *77*, 7–13. [CrossRef]
30. Lund, C.R.F. Effects of zeolite channel walls and cation migration on N_2O decomposition energies in Fe/ZSM-5. *J. Catal.* **2006**, *243*, 438–441. [CrossRef]
31. Fellah, M.F.; Onal, I. N_2O decomposition on Fe- and Co-ZSM-5: A density functional study. *Catal. Today* **2008**, *137*, 410–417. [CrossRef]
32. Mauvezin, M.; Delahay, G.; Coq, B.; Keiger, S.; Jumas, J.C.; Olivier-Fourcade, J. Identification of iron species in Fe-BEA: Influence of the exchange level. *J. Phys. Chem. B* **2001**, *105*, 928–935. [CrossRef]
33. El-Malki, E.; Santen, R.A.; Sachtler, W.M.H. Active sites in Fe/MFI catalysts for NOx reduction and oscillating N_2O decomposition. *J. Catal.* **2000**, *196*, 212–223. [CrossRef]
34. Sobolev, V.I.; Panov, G.I.; Kharitonov, A.S.; Romannikov, V.N.; Volodin, A.M.; Ione, K.G. Catalytic properties of ZSM-5 zeolites in N_2O decomposition: The role of iron. *J. Catal.* **1993**, *139*, 435–443. [CrossRef]
35. Zhang, B.; He, G.; Shan, Y.; He, H. Experimental and DFT study of the adsorption of N_2O on transition ion-exchanged ZSM-5. *Catal. Today* **2019**, *327*, 177–181. [CrossRef]
36. Carlo, L.; Silvia, B.; Mario, S.; Giuseppe, S.; Adriano, Z.; Geobaldo, F.; Vlaic, G.; Bellatreccia, M. XAFS, IR, and UV−Vis study of the Cu^I environment in Cu^I-ZSM-5. *J. Phys. Chem. B* **1997**, *101*, 344–360.
37. Nachtigallova, D.; Nachtigall, P.; Sierka, M.; Sauer, J. Coordination and siting of Cu^+ ions in ZSM-5: A combined quantum mechanics/interatomic potential function study. *Phys. Chem. Chem. Phys.* **1999**, *1*, 2019–2026. [CrossRef]
38. Joshi, A.M.; Delgass, W.N.; Thomson, K.T. Adsorption of copper clusters in TS-1 pores: Ti versus Si and gold versus copper. *J. Phys. Chem. C* **2007**, *111*, 11888–11896. [CrossRef]
39. Bonino, F.; Damin, A.; Ricchiardi, G.; Ricci, M.; Spano, G.; D'Aloisio, R.; Zecchina, A.; Lamberti, C.; Prestipino, C.; Bordiga, S. Ti-Peroxo species in the TS-1/H_2O_2/H_2O system. *J. Phys. Chem. B* **2004**, *108*, 3573–3583. [CrossRef]
40. Pierre, M.; Paul, G.; Robert, S. Understanding the concept of basicity in zeolites. A DFT study of the methylation of Al−O−Si bridging oxygen atoms. *J. Phys. Chem. B* **2006**, *110*, 24947–24954.
41. Joshi, A.M.; Delgass, W.N.; Thomson, K.T. Mechanistic implications of Au_n/Ti-Lattice proximity for propylene epoxidation. *J. Phys. Chem. C* **2007**, *111*, 7841–7844. [CrossRef]
42. Frisch, M.J.; Trucks, G.W.; Schlegel, H.B.; Scuseria, G.E.; Robb, M.A.; Cheeseman, J.R.; Scalmani, G.; Barone, V.; Petersson, G.A.; Nakatsuji, H.; et al. *Gaussian 09, Revision A.02*; Gaussian, Inc.: Wallingford, CT, USA, 2016.
43. Lee, C.; Yang, W.; Parr, R. Development of the Colle-Salvetti correlation-energy formula into a functional of the electron density. *Phys. Rev. B* **1988**, *37*, 785. [CrossRef] [PubMed]
44. Becke, A.D.P. Density-functional exchange-energy approximation with correct asymptotic behavior. *Phys. Rev. A* **1988**, *38*, 3098. [CrossRef] [PubMed]
45. Hansen, N.; Bruggemann, T.; Bell, A.; Keil, F.J. Theoretical Investigation of Benzene Alkylation with Ethene over H-ZSM-5. *J. Phys. Chem. C* **2008**, *112*, 15402–15411. [CrossRef]
46. Ryder, J.; Chakraborty, A.K.; Bell, A. Density Functional Theory Study of Nitrous Oxide Decomposition over Fe- and Co-ZSM-5. *J. Phys. Chem. B* **2002**, *106*, 7059–7064. [CrossRef]

47. Liu, X.; Zhang, J.; Huang, C.; Sun, X. Density Functional Theory Study of Cu-ZSM-5-Catalyzed C–H Bond Activation: The Importance of Active Centers. *J. Phys. Chem. C* **2018**, *122*, 28645–28651. [CrossRef]
48. Trout, B.L.; Chakraborty, A.; Bell, A. Analysis of the thermochemistry of NO_x decomposition over CuZSM-5 based on quantum chemical and statistical mechanical calculations. *J. Phys. Chem.* **1996**, *100*, 17582–17592. [CrossRef]
49. Schneider, W.F.; Hass, K.C.; Ramprasad, R. First-principles analysis of elementary steps in the catalytic decomposition of NO by Cu-exchanged zeolites. *J. Phys. Chem. B* **1997**, *101*, 4353–4357. [CrossRef]
50. Solans-Monfort, X.; Branchaell, V.; Sodupe, M. On the NO decomposition by Cu−ZSM-5 through the $ZCu(NO_2)(NO)$ or $ZCu(N_2O_3)$ intermediates. *J. Phys. Chem. B* **2002**, *106*, 372–1379. [CrossRef]
51. Sengupta, D.; Adams, J.B.; Schneider, W.F.; Hass, K.C. Theoretical analysis of N_2O to N_2 conversion during the catalytic decomposition of NO by Cu-zeolites. *Catal. Lett.* **2001**, *74*, 193–199. [CrossRef]
52. Sierraalta, A.; Bermudez, A.; Rosa-Brussin, M. Density functional study of the interaction of Cu^+ ion-exchanged zeolites with H_2O and SO_2 molecules. *J. Mol. Catal. A* **2005**, *228*, 203–228. [CrossRef]
53. Sierraalta, A.; Anez, R.; Brussin, M. Theoretical study of NO_2 adsorption on a transition-metal zeolite model. *J. Catal.* **2002**, *205*, 107–114. [CrossRef]